

REPORT DOCUMENTATION PAGE

0287

Public reporting burden for this collection of information is estimated to average 1 hour per response, including the time for reviewing instructions, searching existing data sources, gathering and maintaining the data needed, and completing and reviewing the collection of information. Send comments regarding this burden estimate or any other aspect of this collection of information, including suggestions for reducing this burden, to Washington Headquarters Services, Directorate for Information Operations and Reports, 1215 Jefferson Davis Highway, Suite 1204, Arlington, VA 22202-4302, and to the Office of Management and Budget, Paperwork Reduction Project (0704-0188), Washington, DC 20503.

1. AGENCY USE ONLY (Leave Blank)	2. REPORT DATE	3. REPORT TYPE AND DATES COVERED	
	May 29, 1997	Final Report 01 Feb 95 - 31 Mar 97	
4. TITLE AND SUBTITLE		5. FUNDING NUMBERS	
Research on Silicon-Based Optical Devices		61102F 2305/FS	
6. AUTHOR(S)		7. PERFORMING ORGANIZATION NAME(S) AND ADDRESS(ES)	
D. W. Greve Professor of Electrical and Computer Engineering		Carnegie Mellon University Schenley Park Pittsburgh, PA 15213	
8. PERFORMING ORGANIZATION REPORT NUMBER		9. SPONSORING/MONITORING AGENCY NAME(S) AND ADDRESS(ES)	
		AFOSR/NE Building 410 Bolling AFB, DC 20332-6448	
10. SPONSORING/MONITORING AGENCY REPORT NUMBER		11. SUPPLEMENTARY NOTES	
F49620-95-1-0161			
12a. DISTRIBUTION/AVAILABILITY STATEMENT		12b. DISTRIBUTION CODE	
APPROVED FOR PUBLIC RELEASE: DISTRIBUTION UNLIMITED		DTIC QUALITY INSPECTED 2	
13. ABSTRACT (Maximum 200 words)		14. SUBJECT TERMS	
Research on the development of infrared detectors using germanium-silicon alloys is reported. Structures have been grown using ultra-high vacuum chemical vapor deposition (UHV/CVD). Heterojunction internal photoemission structures have been fabricated and characterized. The results suggest that background limited performance will be obtained at 40 K and below for long wave infrared (LWIR) operation. Work on multiple quantum well structures has also been completed and is summarized in the report. Remaining issues concern process integration and some progress is reported toward development of a silicide ohmic contact process to these structures. The growth of relaxed buffer layers and short-period superlattices have also been explored. Most of the results so far have been on short-period superlattices. Characterization by X-ray diffraction and Raman has been performed.		15. NUMBER OF PAGES	
Germanium-silicon, infrared, epitaxial, heterostructure		16. PRICE CODE	
17. SECURITY CLASSIFICATION OF REPORT	18. SECURITY CLASSIFICATION OF THIS PAGE	19. SECURITY CLASSIFICATION OF ABSTRACT	20. LIMITATION OF ABSTRACT
UNCLASSIFIED	UNCLASSIFIED	UNCLASSIFIED	Unlimited

19970616130

Research on Silicon-Based Optical Devices

Final Report¹ AFOSR Contract F49620-95-1-0161

July 31, 1996-March 31, 1997

**D.W. Greve
Department of Electrical and Computer Engineering
Carnegie Mellon University
Pittsburgh, PA**

Research Objectives

This contract supported the development of germanium-silicon growth technology for specific application to infrared sensors. Long-wave infrared (8-12 μm) detectors are of interest for use in focal plane arrays, where integrability with silicon readout circuitry, achievement of background-limited performance, and response uniformity are important. This work was intended to compare two different detector types and to develop a suitable process for fabrication of the more promising design.

Near-infrared detectors (1.3 μm and 1.54 μm) are important for optical fiber links, and here again compatibility with silicon integrated circuit technology is a major reason for investigating $\text{Ge}_x\text{Si}_{1-x}/\text{Si}$ heterostructures. Our goal is to explore the potential of UHV/CVD growth for the fabrication of detectors of this type, especially those using quantum confinement and/or short period superlattices.

Status of the Research Effort- Summary

Long-wave infrared (LWIR detectors) have been characterized. Based on the measured responsivity and dark currents, these detectors are expected to achieve background-limited performance at 8 μm , with some potential for additional improvement as guard rings are incorporated to reduce the dark current. Remaining issues related to process integration are under investigation.

¹ Report period modified by revision of the contract on May 24, 1996 at the request of Major M. Prairie.

The growth of structures suitable for near-IR detectors has been studied. Topics which have received most attention within the report period include the growth of relaxed buffer layers and the growth of short-period superlattices. Complete structures have not yet been grown although some necessary elements have been demonstrated.

Accomplishments and New Findings

Ge_xSi_{1-x} far-IR detectors

A wide variety of detector structures have been explored for focal-plane arrays operating in the far infrared (8-12 μm) region. Of particular interest are detectors made using Ge_xSi_{1-x} which can be grown epitaxially on the same silicon substrates used to fabricate readout circuitry. Possible detector structures include the MQW detector (potentially utilizing either free-carrier or intersubband transitions) and the heterojunction internal photoemission (HIP) detector.

We have grown and characterized these two types of detector structures. MQWs with thresholds appropriate for 8-12 μm operation were found to exhibit only free-carrier absorption in normal incidence. The same absorption mechanism is observed in the HIP structure. We will report the results of optical characterization of HIP detectors which show that background-limited performance can be achieved at operating temperatures near 40 K. In addition, selective growth can be used to grow HIP detectors within contact windows, which permits straightforward integration with the readout circuitry.

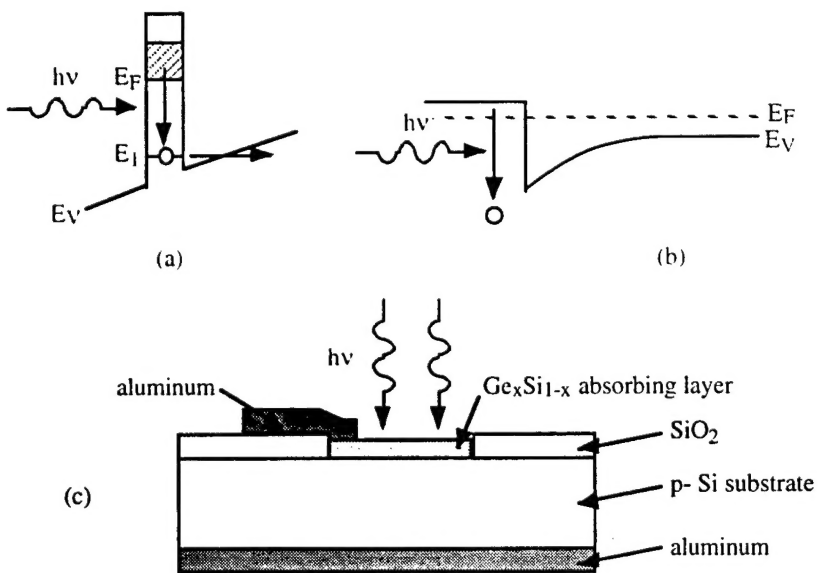


Figure 1. Detector structures: (a) quantum well detector; (b) heterojunction internal photoemission (HIP) detector; and (c) cross section of HIP detector fabricated by selective epitaxial growth.

Figure 1 shows the two different detector structures. In the MQW detector (Fig. 1a), a photocurrent results either from intersubband transitions [1] possibly followed by tunneling (1)

or by free-carrier absorption [2,3] followed by a scattering event which results in the escape of the excited hole from the quantum well (2). The threshold energy is determined by $E_1 - E_F$ or $E_V - E_F$, respectively, and is tailored by choice of the germanium fraction, quantum well thickness, and doping. Figure 1b shows the HIP detector [4-6] in which the absorbing region is thick and the quantum states are very closely spaced. A photocurrent results when free-carrier absorption is followed by a scattering event. Here the threshold energy is $\Psi = E_{V(Si)} - E_F$ and is determined by the germanium fraction of the absorbing layer and the doping concentration.

Uniform epitaxial layers for both detector types were grown by UHV/CVD with threshold energies suitable for 8-12 μm detectors (≈ 0.1 eV). Absorption was characterized by normal-incidence FTIR measurements. Photoresponse measurements were performed on HIP detectors of area 0.036 cm^2 which were fabricated by selective growth in contact windows etched in SiO_2 (Fig. 1c). As we have reported [7], a limited degree of selective growth is possible in UHV/CVD because there is an incubation time before polycrystalline material nucleates on SiO_2 . In addition, dark I(V) measurements were performed in order to determine the Schottky barrier height Ψ .

Epitaxial layers used in this study were grown by UHV/CVD on (100) p-type silicon wafers. We have reported details of the growth technique elsewhere [8]. The MQW structures were grown at 600°C ; before commencing growth of the quantum wells a silicon buffer approximately 1000 \AA thick was grown. HIP structures were grown at 550°C directly on the wafer without a buffer layer (although we found that a cleanup run was necessary in order to reduce residual boron doping in the reactor [9]). Single-pass absorption measurements were performed at room temperature in normal incidence.

Absorption measurements on the MQW structures have been reported briefly already [10] and a more comprehensive data set is available in a thesis [11] and in a paper which has been submitted [12]. Briefly, in normal incidence we observe peaked absorption only in samples with doped buffer layers. The peak positions were uncorrelated with the predicted positions of intersubband transitions but were consistent with interference due to reflections from the doped buffer layer [10]. Thus the only significant absorption attributable to holes in the quantum wells is the monotonically increasing free carrier absorption. This is in agreement with a recent report by Robbins et al. [3], but not with an earlier report by People et al. who observed peaked absorption in MBE-grown structures [13].

Figure 2 shows the measured absorption for $\text{Ge}_{0.38}\text{Si}_{0.62}$ layers with thicknesses typical of those used in HIP detectors. Thicknesses and doping concentrations were measured by secondary ion mass spectrometry. Again free-carrier absorption monotonically increasing with wavelength is observed. Details of these experiments and the further characterization of HIP detectors are available in another thesis [14]; what follows is a brief summary of those results. As we have previously reported [15], analysis of the data shows that not all of the boron is electrically active for the more heavily doped samples and that the maximum electrically active boron concentration is approximately $3.3 \times 10^{20} \text{ cm}^{-3}$.

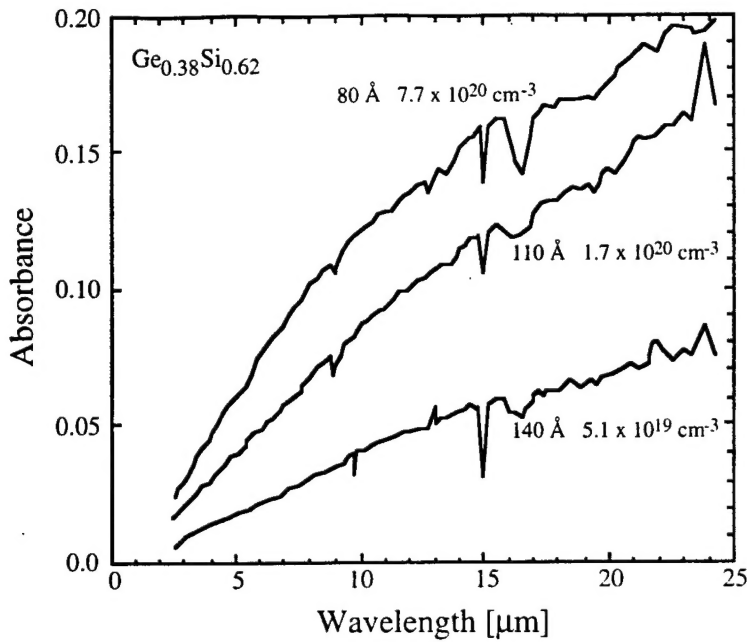


Fig. 2. Normal incidence FTIR measurements on layers for HIP detector fabrication.

The free carrier absorption mechanism depends only on the number of carriers and the scattering rate; thus it will be observed in *any* heavily doped GeSi layer, regardless of thickness. The scattering rate $1/\tau$ can be extracted from the transmission measurements using the classical expression for free-carrier absorption

$$ABS = -\log_{10}(I_{\text{incident}}/I_{\text{transmitted}}) = 0.434[2N_A N t_{\text{well}} q^2 \tau / (1 + \omega^2 \tau^2) m * c \epsilon_0 n_o]$$

in which N_A is the doping concentration, t the layer thickness, and n_o the index of refraction. For the quantum well structures we obtain $\tau \approx 10^{-14}$ sec [12] while for the more heavily doped HIP structures $\tau \approx 5 \times 10^{-15}$ sec. [12]. The absorption per hole is greater in the HIP structures and in addition the doping concentration is considerably greater.

The relative performance of HIP and MQW detectors depends on the achievable responsivity R [amperes/watt] and dark current-induced noise ($i_n^2 \sim I_{\text{dark}}$). A high responsivity and low current noise is desirable in order to maximize the detectivity D^* . We have used the measured absorption to compare the potential performance of HIP and MQW detectors under the assumption that all carriers energetically able to surmount the barrier in fact contribute to the observed current [12]. This overestimates the photocurrent, but at least in the MQW detector measurements show that the assumption that the probability of escape is unity is not too far from correct, at least with high applied fields [3]. With this assumption, HIP detectors are expected to have better sensitivity by roughly a factor of three. HIP detectors are also expected to have higher D^* values unless a large number of quantum wells are used; this is because responsivity is independent of the number of wells while noise decreases as the number of wells increases [16].

On the basis of this analysis, we chose to further examine the HIP detector, as it appeared to offer high responsivity, acceptable D^* , and a process highly compatible with silicon

readout circuitry.² A critical issue was the measurement of the *actual* probability of escape of excited carriers in the HIP structure, and also determination of the dark currents in real structures.

Characterization of HIP Detectors

The threshold energy for a HIP detector is given by the expression

$$\Psi = \Delta E_V(\text{Ge}) + \Delta E_V(\text{B}) - (E_V - E_F)$$

where $\Delta E_V(\text{Ge})$ is the valence band offset, $\Delta E_V(\text{B})$ the heavy-doping bandgap narrowing, and $(E_V - E_F)$ is the bandfilling due to electrically active boron. The first term depends only on the germanium fraction x ; the second terms depend on the boron concentration but with opposite sign. Generally the highest electrically active boron concentration possible is used and x is adjusted to obtain the desired threshold. The dependence of bandgap narrowing on boron concentration is not well known in $\text{Ge}_x\text{Si}_{1-x}$; as a result the germanium fraction must be determined experimentally.

sample	x	N_A [cm ⁻³]	Ψ [eV] (electrical)	Ψ [eV] (optical)	C_1 [%/eV]
E	0.50	2.5×10^{20}	0.15	0.15	14
F	0.42	3.0×10^{20}	0.14	0.15	21
G	0.38	6.5×10^{20}	0.12	0.13	20
H	0.30	3.0×10^{20}	0.10	0.10	18

Table I. Parameters of several HIP structures examined in this study.

Table I presents the germanium fraction and other parameters for several HIP structures with thresholds near $\Psi=0.10$ eV. Typical reverse $I(V_A)$ characteristics for sample H are shown in Fig. 3. The reverse current is thermally activated for temperatures above 42 K. Fitting the measured reverse current at $V_A=1$ V to the usual expression $I=qA*T^2e^{-\Psi/kT}$ yields the electrical barrier height shown in Table I.

² Use of an MQW detector with a large number of wells would result in a highly nonplanar surface incompatible with standard integrated circuit processes. In addition, passivation of the detector edges would be required. In contrast, the HIP detector structure can be selectively grown within a contact window, using a process very similar to that presently used for mid-IR PtSi detectors.

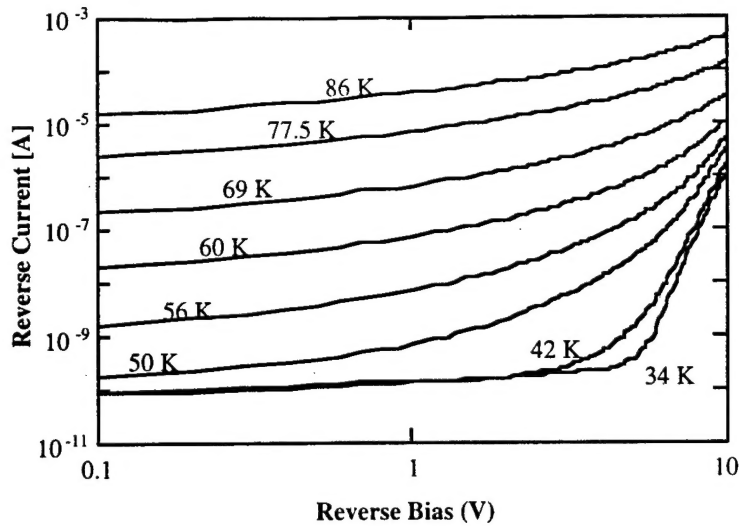


Fig. 3. Measured dark reverse currents for sample H as a function of temperature.

Optical measurements were performed at 40 K using a glowbar IR source, a monochromator and phase-sensitive detection. The photocurrent is expected to follow the modified Fowler form

$$Y[\%] = (\text{collected electrons})/(\text{incident photons}) \times 100\% = C1(hv - \Psi)^2/hv.$$

Figure 4 shows the results of these measurements for sample H. The data follow the Fowler form near threshold; extrapolation yields the optical barrier height, also presented in Table I. Above threshold, the data falls below the Fowler form; in this range the data can be fit reasonably well by a theory which takes account of the dependence of absorption on wavelength and the details of the densities of initial and final states [14]. Table I shows that there is good agreement between the electrical and optical barrier heights and that thresholds in the range desired have been obtained. As expected, Ψ decreases with decreasing germanium fraction x . The $C1$ values obtained are similar to those obtained for PtSi detectors operating in the 3-5 μm region.

As noted above, it is of particular interest to achieve background-limited infrared performance (BLIP) in which the dark current-induced noise is less than the noise due to fluctuations in the number of incident photons. This will be achieved when the detectivity $D^* > 6 \times 10^{10}$ at 8 μm with a 300 K background. Assuming full shot noise, the detectivity is given by

$$D^* = (Aq/2)^{1/2} (Y/hv I_{\text{dark}})^{1/2}$$

where A is the detector area. Using the measured dark current at $V_A = -1\text{V}$ yields $D^* = 7 \times 10^{10}$ at 8 μm for detector H. For this sample, at 40 K the dark current at -1 V is due to edge currents, so it is likely that this can be improved somewhat by using a process with guard rings. A further improvement of approximately a factor of two will result by using an optical cavity.

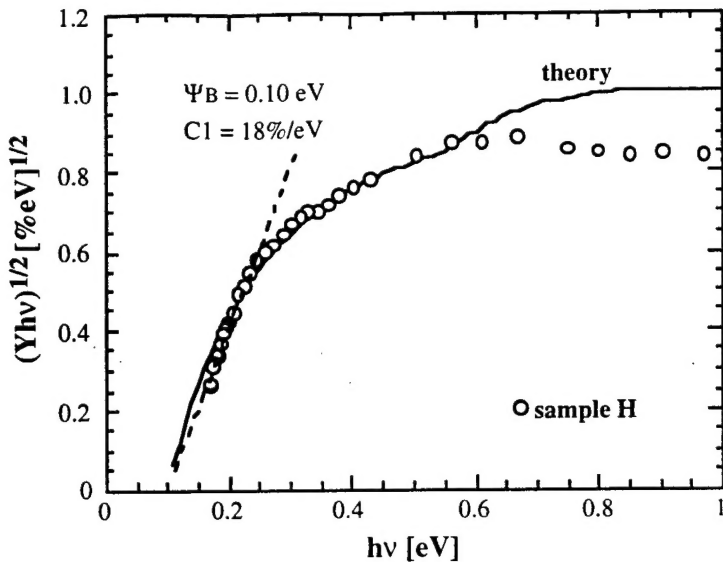


Fig. 4. Fowler plot of the yield for sample H (data points) and theoretical prediction (solid line).

The measurements of responsivity on these detectors and others have been used to determine the probability of escape of excited carriers. These measurements will shortly be reported in another paper [17]. Briefly, the probability of escape is comparable to that of MQW detectors measured with moderate applied fields (a condition which will be required in actual operation to minimize dark currents in the MQW design).

Process Integration

We have shown above that the HIP detector offers the attractive combination of an integrable process and good performance. Major unresolved issues are (1) the further reduction of the dark current and (2) development of a more suitable contact technology.

The dark current can be effectively reduced by the introduction of guard rings. We have grown HIP structures on wafers provided by P. Pellegrini which incorporate guard ring structures. Measurements on these devices show a great reduction in dark current, although the responsivity of these detectors was not as high as those previously measured [18]. This may be due to different illumination conditions (rear illumination as opposed to front illumination). This issue should be resolved in studies planned for the near future.

It is also necessary to improve the contact technology to the front surface. So far we have used aluminum contacts with an annealing temperature carefully adjusted to provide a good ohmic contact without spiking. A more manufacturable solution would be to use a silicide where the silicidation reaction consumes a predictable amount of material.

In recent work, we have examined the possibility of using cobalt silicide. This particular material was suggested to us based on success in applying it to thin film transistors (M.K. Hatalis, private communication). There are similar requirements in HIP structures since we wish to make an ohmic contact with minimal consumption of silicon.

Results obtained prior to the contract end date were encouraging but incomplete. Substantial difficulty was encountered initially, due to oxidation both at the cobalt-silicon interface and also during annealing to form the silicide. Oxidation at the interface was expected and was addressed using HF-last clean and also presputtering. Oxidation during annealing was also a substantial problem, even when using rapid thermal annealing in a nitrogen ambient. In the end encouraging results were obtained with an *in situ* anneal in vacuum. In this way resistivities close to cobalt silicide bulk resistivities were obtained.

Near-IR detector designs

We have initiated the exploration of several possible designs for near-IR detectors using germanium-silicon epitaxial growth. We report below progress to date on two different types of detectors:

1. Multiple quantum well detectors using strained Ge_xSi_{1-x} or GeSiC wells grown on silicon substrates. This type of detector was first proposed by Temkin and coworkers [19] and later studied by other groups. The main problem with this type of detector is the weak absorption in the well regions. The absorption can be increased by increasing either the well width or the germanium fraction but the degree to which this can be done is limited by critical thickness and the onset of undulation formation.

One possible solution is to allow the undulations to develop resulting in the formation of quantum dots. Much recent research has suggested that there is an increase in absorption strength in quantum-confined regions.

We have examined the possibility of inducing undulations by introducing a growth interruption after growth of the Ge_xSi_{1-x} layer. Samples with and without a growth interruption have been grown and fabricated into pin device structures. The observed leakage currents were quite high and X-ray diffraction measurements suggest that all samples are partially relaxed, suggesting that the germanium fraction was too high. Limited time prevented us from exploring this any further in this contract.

As noted above, the critical thickness limitation is a major problem. A possible solution is to use GeSiC quantum wells which can be grown to greater thickness for a given bandgap difference.

2. Superlattice structures. The possibility of a quasi-direct gap in germanium-silicon short period superlattices was predicted early on [20] and despite some encouraging experiments has remained controversial. The quality of the superlattices has always been an issue because very low growth temperatures or surfactants are required in MBE growth, leading to the probably incorporation of defects or impurities. We have explored the growth of these structures by UHV/CVD, where hydrogen acts as a surfactant without any incorporation into the film.

Growth of these structures involves two aspects: the growth of a relaxed buffer layer and then growth of the short-period superlattice itself. We have examined these two steps

separately. Graded buffer layers have been grown both at high (750 °C) and low (550 °C) temperature. Briefly, low temperature buffers were grown with a grading rate of 20%/ 1000 Å. These buffers were only partially relaxed as determined by X-ray diffraction. In contrast, high temperature buffer layers with a grading rate of 6%/ 1000 Å were closer to being fully relaxed, as determined by reciprocal space mapping [21]. However, these layers are quite rough and thus it is not possible to use Raman spectroscopy to study the quality of superlattices grown on them. Possibilities include the use of lower grading rates for the low-temperature buffers (at the price of longer growth time) and polishing of the high temperature buffers after growth.

We have also performed separate experiments to examine the possibility of growth of small numbers of monolayers by UHV/CVD. In order to avoid complications associated with the buffer layer, we grew thin (3-5 Å) germanium layers and relatively thick silicon layers (20-30 Å). While the period is not as short as required for the detector structures, these still represent the shortest periods yet reported using a CVD growth technique. This work was reported at a recent conference [21].

Si/Ge superlattices with periods of about 30 Å have been grown at temperature set points of 520° C and 475° C (see Table II) and have been characterized by high resolution X-ray diffraction, grazing incidence X-ray reflectivity and Raman spectroscopy.

The (004) X-ray diffraction spectra for all the samples are shown in Fig.5. All the samples produced superlattice peaks that give information on average composition and periodicity of the multilayers. The individual layer thickness in each superlattice presented in Table II is a result of dynamical simulations of the (004) diffraction spectra. Samples B and C have well defined thickness fringes around the main superlattice peak. For sample A the thickness fringes are absent. This could be due either to destructive interference caused by thickness fluctuations or to an increase in the diffusely scattered radiation from misfit dislocations. Sample A has the highest Ge layer thickness, 7.6 Å, significantly above the critical thickness for islanding and for strain relaxation for pure Ge and thus both thickness fluctuations and misfit dislocations could be present. Although misfit dislocations may be present they did not produce a significant strain relaxation as the in plane average lattice constant was measured to be the same as for the Si substrate within experimental error.

Sample	growth temperature	Ge thickness [Å]	period [Å]
A	475° C	34	7.6
B	475° C	27.5	5.2
C	520° C	25.5	4.8

Table II. Growth temperature, period and Ge layer thickness for the samples studied. Period and Ge layer thickness were found from dynamical simulations of (004) ω -2θ diffraction spectra.

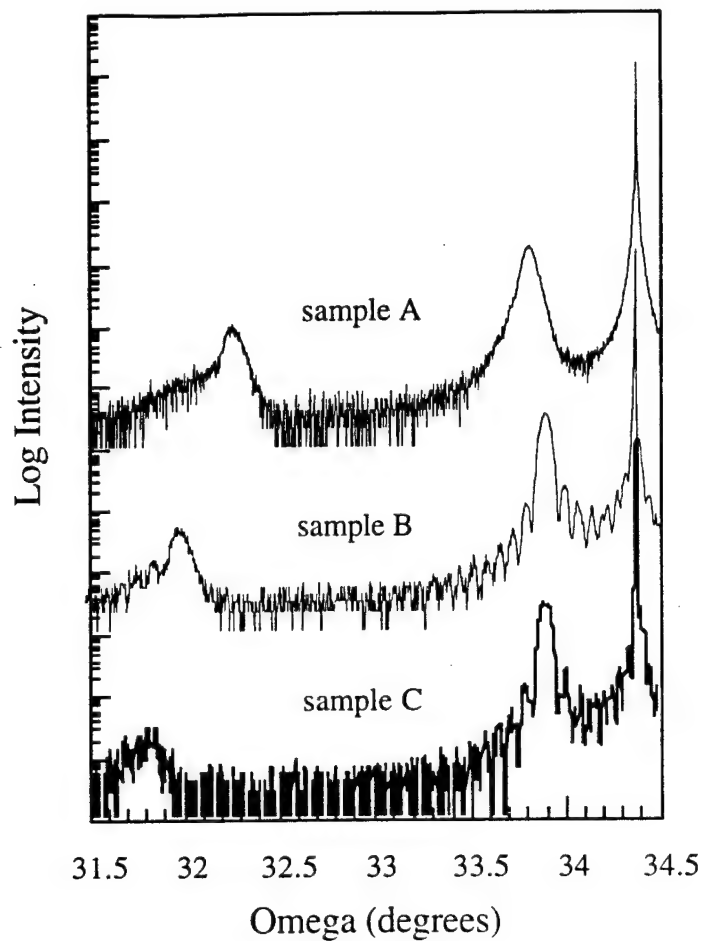


Fig. 5. (004) HRXRD spectra of samples A,B,C. Samples B and C exhibit thickness fringes while sample A does not.

Low angle of incidence X-ray reflectivity measurements are less sensitive to the crystalline quality of the material but they provide information on the interface planarity and intermixing. Specular reflectivity spectra for the three samples studied are shown in Fig.6. Comparing spectra for samples B and C one notices that the first order satellite (the peak at $\approx 2.5 \text{ nm}^{-1}$) has a higher intensity and is accompanied by thickness fringes in sample B. This is indicative of more planar interfaces and lower intermixing in the sample grown at 475° C . Lower growth temperature results in a reduction in Si and Ge interdiffusion and in Ge surface segregation but also in an increase in hydrogen surface coverage. Hydrogen acts as a surfactant in UHV/CVD growth kinetically inhibiting Ge segregation and islanding.

Sample A exhibits the strongest first order satellite. This effect is caused by an increased contrast between the electron densities of the alternating layers in the superlattice. Sample A has the highest amount of Ge in a period therefore the electron density contrast between the highest and lowest Ge fraction in a period is improved leading to increased intensity of the satellite.

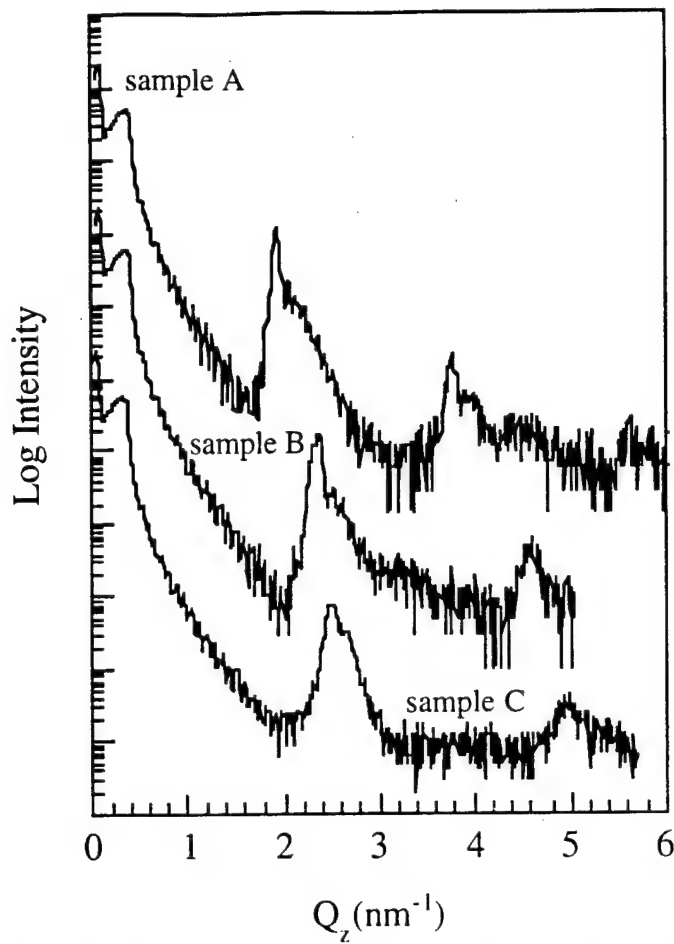


Fig. 6. Specular reflectivity spectra of samples A,B,C. Sample A has the strongest first order satellite. Thickness fringes around first order satellite are absent in sample C indicating poor interfaces..

In order to determine the presence or absence of islands in these samples reciprocal space scans across the first feature in specular reflectivity spectra have been taken. The side peaks in the diffuse scattered intensity around specular Bragg peaks characteristic of island formation have not been observed for our samples and we conclude that islands with periodicity in the 1500 Å to 2 μm range are not present.

Finally, the Raman spectrum of Sample A is shown in Fig.7. It exhibits a strong folded acoustic phonon peak that corresponds to the periodicity of the SL. The spectra for samples B and C are more alloy-like and the folded acoustic phonon peak has not been observed. Si-Ge peaks are strong compared to Si-Si and Ge-Ge peaks for all samples suggesting significant interface intermixing.

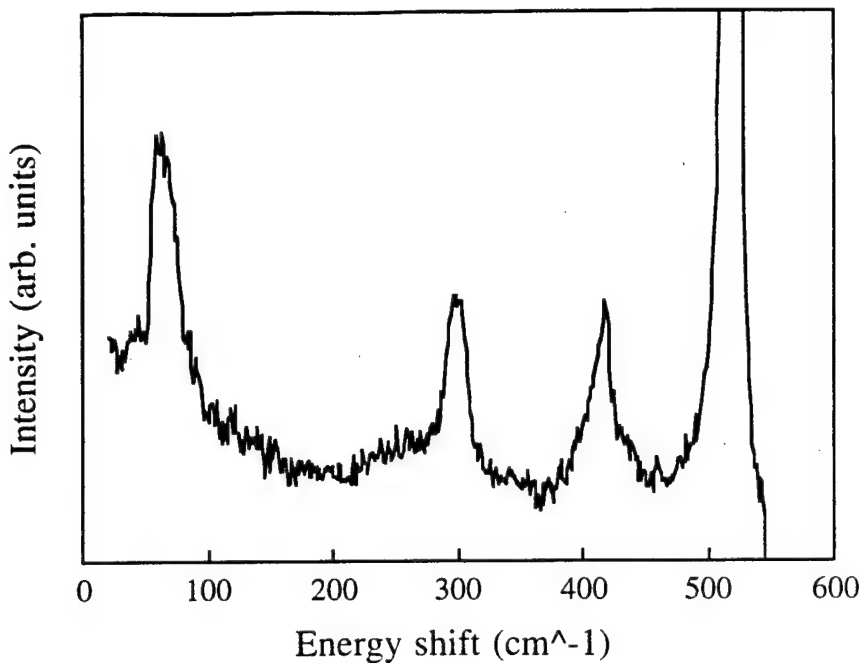


Fig. 7. Raman spectra of sample A.
A strong folded acoustic phonon peak is visible at $\approx 60 \text{ cm}^{-1}$.

In conclusion, we have studied the effect of growth temperature and Ge layer thickness in UHV/CVD grown short period superlattices. Lower growth temperature improves the interface quality as shown by X-ray reflectivity measurements. The sample with a larger Si and Ge layer thickness has shown a better defined period and improved Ge concentration contrast. However, all samples are strongly intermixed as evidenced by Raman experiments. For growth of shorter period superlattices further reduction in intermixing has to be obtained by lowering the growth temperature.

Summary

We regard our work on LWIR detectors as a significant success. Growth of aggressive structures with very thin layers and high doping has led us to further develop the UHV/CVD growth technique. Problems encountered during growth have been solved and we have a much greater understanding of the growth process itself. This will be of substantial benefit to other groups applying UHV/CVD or CVD of GeSi in general.

Detector structures have been fabricated and characterized. We strongly support the HIP detector as an alternative to the QWIP detector in the 8-12 μm region, for a number of reasons that have to do with detector performance in normal incidence and also process compatibility. The results suggest that background-limited performance will be obtained at 40 K and below. In addition, our model for the photoresponse strongly suggests that the detectors fabricated here are near optimum in performance.

Work on near-IR detectors has been cut short by program cancellations. However, the

results obtained so far show that UHV/CVD can be pushed to smaller structures than previously thought, that is, nearly to the short-period superlattice regime. This is a surprising result for a multi-wafer growth technology.

References

1. J.S. Park, R.P.G. Karunasiri, and K.L. Wang, *Appl. Phys. Lett.* **60** (1992) 103.
2. J.S. Park, R.P. G. Karunasiri, and K.L. Wang, *Appl. Phys. Lett.* **61** (1992) 681.
3. D.J. Robbins, M.B. Stanaway, W.Y. Leong, R.T. Carline, N.T. Gordon, *Appl. Phys. Lett.* **66** (1995) 1512.
4. F.D. Shepherd Jr., V.E. Vickers, and A.C. Yang, US Patent 3603847 (1971).
5. T.L. Lin and J. Maserjian, *Appl. Phys. Lett.* **57** (1990) 1422.
6. J.S. Park, T.L. Lin, E.W. Jones, H.M. Del Castillo, and S.D. Gunapala, *Appl. Phys. Lett.* **64**, 2370 (1994).
7. M. Racanelli and D.W. Greve, *Appl. Phys. Lett.* **58** (1991) 2096.
8. R. Misra, R. Strong, D.W. Greve, and T.E. Schlesinger, *J. Vac. Sci. Technol.* **B 11** (1993) 1106.
9. S. Vyas, D.W. Greve, T.J. Knight, R.M. Strong, and S. Mahajan, *Vacuum* **46** (1995) 1065.
10. R. Misra, D.W. Greve, and T.E. Schlesinger, *Appl. Phys. Lett.* **67** (1995) 2548.
11. R. Misra, unpublished Ph.D. thesis, (Carnegie Mellon University, 1995).
12. R. Strong, R. Misra, D.W. Greve, and P.C. Zalm, (revised version under review for *Journal of Applied Physics*).
13. R. People, J.C. Bean, C.G. Bethea, S.K. Sputz, L.J. Peticolas, *Appl. Phys. Lett.* **61**, 1122 (1992).
14. R.M. Strong, unpublished Ph.D. thesis, (Carnegie Mellon University, 1996).
15. R. Strong, D.W. Greve, T.E. Schlesinger, M.M. Weeks, and P. Pellegrini, in *Proc. MRS Symposium C on Strained Layer Epitaxy- Materials, Processing, and Device Applications* pp. 339-44, (Materials Research Society, Pittsburgh, PA, USA, 1995).
16. H.C. Liu, *Appl. Phys. Lett.* **61**, 2703 (1992).
17. R.M. Strong, D.W. Greve, M.M. Weeks, and P. Pellegrini, (revised version under review for *Journal of Applied Physics*).
18. M. Weeks, private communication.
19. H. Temkin, J.C. Bean, T.P. Pearsall, N.A. Olsson, and D.V. Lang, *Appl. Phys. Lett.* **49**, 155 (1986).
20. U. Gnutzman and K. Clausecker, *Appl. Phys.* **3**, 9 (1974).
21. D.W. Greve and A.C. Mocuta (American Vacuum Society Meeting, October, 1996, Philadelphia, PA).

Publications

Book Chapter

Ge_xSi_{1-x} Epitaxial Growth and Application to Integrated Circuits," invited book chapter in *Physics of Thin Films*, Volume 23 (Academic Press, 1997).

Journal Articles

"Growth of Epitaxial Ge_xSi_{1-x} for Infrared Detectors by UHV/ CVD," S. Vyas, D.W. Greve, T.J. Knight, R.M. Strong, and S. Mahajan, *Vacuum* **46**, 1065 (1995).

"Infrared Absorption in Ge_xSi_{1-x} Quantum Wells, R. Misra, D.W. Greve, and T.E. Schlesinger, *Appl. Phys. Lett.* **67**, 2548 (1995).

" Ge_xSi_{1-x} Epitaxial Growth and Application to Integrated Circuits," invited book chapter to appear in *Physics of Thin Films*, Volume 21, (Academic Press; M.H. Francombe, editor).

" Ge_xSi_{1-x} far-infrared detectors I: absorption in multiple quantum well and heterojunction internal photoemission structures," R. Strong, R. Misra, D.W. Greve, and P.C. Zalm (revised version presently under review for *J. Appl. Phys.*).

" Ge_xSi_{1-x} far-infrared detectors II: characterization of heterojunction internal photoemission detectors," R.M. Strong, D.W. Greve, M.M. Weeks, and P. Pellegrini (revised version presently under review for *J. Appl. Phys.*).

Conference Proceedings

" Ge_xSi_{1-x} Heterojunction Internal Photoemission Structures by Ultra- High Vacuum Chemical Vapor Deposition," R. Strong, D.W. Greve, T.E. Schlesinger, M.M. Weeks, and P. Pellegrini, (to appear in *Proc. MRS Symposium C on Strained Layer Epitaxy- Materials, Processing, and Device Applications*).

" Ge_xSi_{1-x} infrared detectors grown by ultrahigh- vacuum chemical- vapor deposition for focal- plane arrays," R. Strong, D.W. Greve, T.E. Schlesinger, M. Weeks, and P. Pellegrini, (extended abstract in CLEO 1995 Technical Digest, pp. 357- 358).

"GeSi Infrared Detectors using Selective Deposition," R. Strong, D.W. Greve, M.M. Weeks, to appear in Proc. MRS Symposium H, (Boston, MA, December, 1995).

Invited Presentations

"Growth and Optimization of Ge_xSi_{1-x} Heterostructures for Long-wave infrared Detectors," D.W. Greve, Workshop on GeSiC Alloys, (April, 1997, Austin, TX).

Seminars and Conference Presentations

“Germanium-Silicon Strained-Layer Epitaxy and Applications,” Seminario, Seccion Estado Solido, Departamento de Fisica, Centro de Investigacion y de Estudios Avanzados del Instituto Politecnico Nacional, Mexico City, Mexico (March 22, 1995).

“ Ge_xSi_{1-x} Heterojunction Internal Photoemission Structures by Ultra-High Vacuum Chemical Vapor Deposition,” R. Strong, D.W. Greve, T.E. Schlesinger, M.M. Weeks, and P. Pellegrini, 1995 Spring MRS Meeting, (San Francisco, CA, March, 1995).

“GeSi Infrared Detectors using Selective Deposition,” R. Strong, D.W. Greve, M.M. Weeks, presented at MRS Fall Symposium H, (Boston, MA, December, 1995).

“Low Temperature Epitaxial Growth of Silicon and Ge_xSi_{1-x} ,” seminar at Westinghouse Advanced Technology Laboratory, (Baltimore, MD, July 3, 1995).

“ Ge_xSi_{1-x} infrared detectors grown by ultrahigh-vacuum chemical-vapor deposition for focal-plane arrays,” R. Strong, D.W. Greve, T.E. Schlesinger, M. Weeks, and P. Pellegrini, Photodetectors: MWIR to UNIR, CLEO 1995, (Baltimore, MD, May, 1995).

“GeSi Infrared Detectors, D.W. Greve, R. Strong, M. Weeks, and P. Pellegrini, Symposium F: GeSi and Related Compounds, Materials Research Society Spring Meeting (San Francisco, CA, April, 1996).

“ Ge_xSi_{1-x} far infrared detectors,” R. Strong, D.W. Greve, R. Misra, M. Weeks, and P. Pellegrini, (Symposium D: Group IV Heterostructures, European Materials Research Society, Strasbourg, France, June, 1996).

“Application of quadrupole mass spectrometry for fault detection in an epitaxial growth process,” D.W. Greve and R. Strong, AEC/APC Workshop VIII, (October 27-30, 1996, Santa Fe, NM).

“Growth of short period superlattices by chemical vapor deposition,” D.W. Greve and A.C. Mocuta, presented at the American Vacuum Society Meeting, (October, 1996, Philadelphia, PA).

“Growth and optimization of Ge_xSi_{1-x} heterostructures for far infrared detectors,” Rome Laboratory, Hascom AFB, MA, September 30, 1996.

“Growth and optimization of Ge_xSi_{1-x} heterostructures for far infrared detectors,” Electronic Materials Seminar, MIT, Cambridge, MA, October 1, 1996.

“Growth and optimization of Ge_xSi_{1-x} heterostructures for far infrared detectors,” informal seminar, Department of Physics and Measurement Technology, Linköping University, Linköping, Sweden (October, 1996).

"Extending silicon integrated circuit technology with germanium-silicon epitaxy," Department of Electrical Engineering Seminar, University of Pittsburgh. (February 3, 1997, Pittsburgh, PA).

Ph.D. Theses

"Germanium-Silicon Quantum Well Infrared Photodetectors," R. Misra, (unpublished Ph.D. thesis, Carnegie Institute of Technology, 1995).

"Germanium Silicon Infrared Detectors by Ultra High Vacuum Chemical Vapor Deposition," R.M. Strong, (unpublished Ph.D. thesis, Carnegie Institute of Technology, 1995).

Personnel

Faculty

D.W. Greve, Professor ECE, principal investigator

Graduate Students

S. Vyas (M.S. received 1994).
R. Misra (Ph.D. received 1995).
R. Strong (Ph.D. received 1996).
J. Ganong (M.S. received 1997).
A. Mocuta (Ph.D. in progress)

Interactions

There has been an ongoing interaction with Rome Laboratory at Hanscom AFB. Examples include the following:

- measurements at Rome of detector structures fabricated at CMU
- growth at CMU of GeSi layers on partially processed wafers provided by Rome Laboratory; subsequently completed and successfully measured at Rome Laboratory;
- consultation with Rome personnel in the course of the design, specification, and initial testing of a UHV/CVD system at Rome Laboratory;
- visit to Rome Laboratory by R.M. Strong to discuss work on HIP detectors; and
- a number of joint conference presentations and journal articles resulting from this work; and
- visit to Rome Laboratory by D.W. Greve to summarize work on HIP detectors.

There is also growing interaction with Northrup-Grumman (division which was formerly Westinghouse). Examples include:

- a grant to CMU to study process diagnostics and control of the UHV/CVD reactor;
- CMU participation as a subcontractor on the MAFET program (program objectives are HBT fabrication; start date October 1); and
- CMU interactions with a supplier (Epigress AB) who will provide a commercial UHV/CVD system to Northrup-Grumman.

Inventions/ Patent Disclosures

None to date.